Criteria for Recognition of Subducted (Orocopia) Schist in Western Arizona

G. B. Haxel[1], J. S. Singleton[2], C. E. Jacobson[3], N. M. Seymour[4], J. E. Spencer[5], E. D. Strickland[2], and L. S. Beard[6]

[1]USGS, Flagstaff, AZ; Northern Arizona University, Flagstaff, AZ; gbhcjh@gmail.com
[2]Colorado State University, Fort Collins, CO
[3]Iowa State University, Ames, IA; University of Pennsylvania, West Chester, PA
[4]Stanford University, Stanford, CA
[5]University of Arizona, Tucson, AZ
[6]USGS, Flagstaff, AZ

Orocopia Schist Subduction Channel, Southwest Arizona

The Orocopia Schist is a latest Cretaceous low-angle subduction channel, part of a larger subduction complex, the Pelona-Orocopia-Rand Schist (PORS), that underlies much of southern California and southwest Arizona (Fig. 1; Jacobson et al. 1988, 2007, 2011; Haxel et al. 2002; Chapman 2016). The principal locus of Orocopia Schist, the Chocolate Mountains anticlinorium extending from the Orocopia Mountains east to Neversweat Ridge, has been known since the mid 1970s (Haxel and Dillon 1978). Recently, two more exposures of the oceanic Orocopia Schist have been found at isolated localities farther inland in southwest Arizona: Cemetery Ridge (Haxel et al. 2015, 2018b, 2021; Jacobson et al. 2017) and northern Plomosa Mountains (Strickland et al. 2017, 2018; Seymour et al. 2018). These discoveries raise the possibility that additional inboard areas of Orocopia Schist have yet to be found. Hence a review of criteria for recognition of Orocopia Schist is warranted.

Positive Criteria

P1—Homogeneous quartzofeldspathic schist—metamorphosed turbidite sandstone—with planar schistosity parallel to transposed bedding (Fig. 2A, B).

P2—Porphyroblasts of bluish-gray to black graphitic plagioclase (Fig. 2C).

P3—Metamorphic biotite ± accessory garnet in quartzofeldspathic schist (Fig. 2D).

P4—Sparse layers of morb-like metabasalt, most commonly with flattish (T-morb–like) chondrite-normalized REE spectra (Fig. 3).

P5—Sparse layers of ferromaganiferous metachert (magnetite-spessartine quartzite) and siliceous marble; REE spectra have negative Ce anomalies inherited from seawater (Fig. 4).

P6—Pods of coarsely bladed high-Cr and -Ni actinolitite, produced by inteaction of subducting schist with peridotite (Fig. 5).

P7—Pods or blocks of serpentinite, calc-serpentinite, or peridotite (rare).

P8—Detrital-zircon age spectra with Paleoproterozoic, Mesoproterozoic, Jurassic, and Late Cretaceous peaks (Fig. 6).

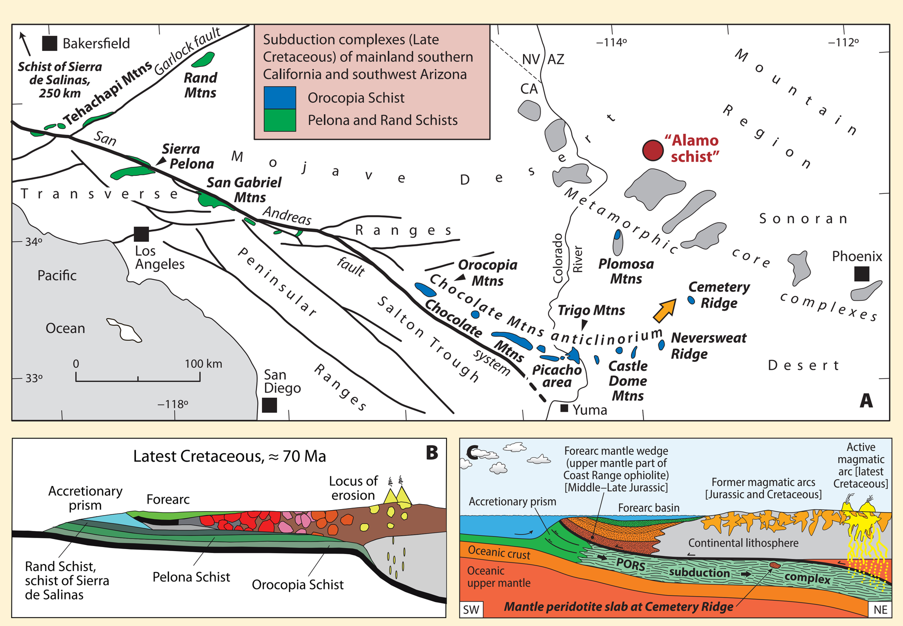

Figure 1. (A) Distribution of Orocopia Schist, and correlative Pelona and Rand Schists (collectively PORS), southern California and southwest Arizona, showing recently discovered exposures of Orocopia Schist at Cemetery Ridge and in the Plomosa Mountains, relative to the main locus of Orocopia Schist, the Chocolate Mountains anticlinorium. Orange arrow marks approximate direction of subduction of PORS, inferred from the orientation of prograde metamorphic lineation (Haxel et al. 2018a). Map updated from Haxel et al. (2002); metamorphic core complexes after Spencer and Reynolds (1989a, 1990). **(B, C)** Cartoons illustrating low-angle subduction model for PORS (after Grove et al. 2003, Haxel et al. 2015).

Negative Criteria

N1—*Sedimentary or volcanic features visible in hand specimen: sand grains, pebbles, quartz or feldspar phenocrysts, lithic fragments, pumice lapilli, or eutaxitic foliation.*

N2—Pelitic rocks.

N3—Quartzite derived from quartz arenite.

N4—Banded iron formation or associated ferruginous metachert.

N5—Pre-Cenozoic igneous intrusions.

Not Orocopia Schist, Regional

Regional or local units that fail several or most of these criteria include: (1) Proterozoic metasedimentary rocks in the Harcuvar-Buckskin core complex, Bouse Hills, and hills west of Tonopah. (2) Metamorphosed Paleozoic and Triassic strata. (3) Metamorphosed Jurassic and Cretaceous sedimentary, volcanic, volcaniclastic, and hypabyssal rocks widespread in southwest Arizona.

Not Orocopia Schist: "Alamo Schist"

Elliott and Corones (2019) suggest that schistose rocks along Alamo Crossing Road northeast of the Rawhide Mountains (Fig. 1; Bryant 1995) are Orocopia Schist. However, this so-called "Alamo schist" fails all of criteria P1 to P8—it lacks the oceanic character of Orocopia Schist. Equally important, the "Alamo schist" decisively fails N1. The specific rock mistaken for Orocopia Schist is a loose block, beside the road, of dark-gray metarhyolite (Fig. 7A, B, C). This block lies within, and is presumably part of, a fault-bounded sliver of Miocene megabreccia, probably rock-avalanche or debris-flow breccia (Fig. 8; Lucchitta and Suneson 1989, 1994; Spencer and Reynolds 1989; Spencer et al. 1989; Yarnold 1989; Yarnold and Lombard 1989). Surrounding outcrops within the breccia unit are light-gray metamorphosed rhyolitic lithic tuff and tuffaceous sandstone (Fig. 7D), sericitic and weakly to moderately foliated. All these low-grade metamorphic rocks have prominent remnant quartz phenocrysts (Fig. 7B). None contain graphitic plagioclase or metamorphic biotite. Our field examination and comprehensive map-unit description by Lucchitta and Suneson (1994) and Bryant (1995) provide no evidence for presence of Orocopia-like metabasalt, Fe-Mn metachert or marble, or actinolitite. Several other features described by Elliott and Corones (2019) are likewise consistent with sedimentary or tectonic breccia but inconsistent with Orocopia Schist.

The spectrum of U-Pb zircon ages from the dark metarhyolite comprises a single peak at 160–180 Ma, centered on 167 Ma (Elliott and Corones 2019). Jurassic igneous and meta-igneous rocks are common in southwest Arizona and southeast California. The metarhyolite lacks zircon of other ages characteristic of Orocopia (meta)sandstone (Fig. 6) because the analyzed rock is not sedimentary.

Conclusion

In correctly identifying Orocopia Schist, both positive and negative criteria are important. We hope the information summarized here can further the search for additional exposures of subducted schist in western Arizona by averting any more false positives.

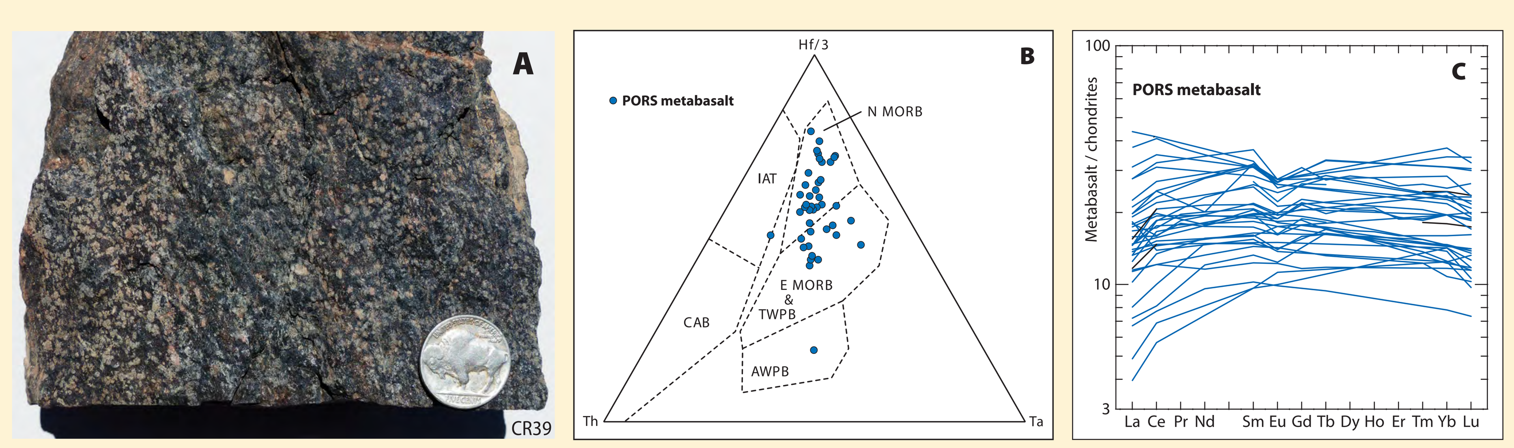

Figure 3. PORS metabasalt. **(A)** Weathered surface of medium-grained schistose amphibolite, composed of black acicular hornblende, white porphyroblasts of calcic andesine, and minor diopside and titanite (not visible); Orocopia Schist, Cemetery Ridge, southwest Arizona. Diopside is atypical, and owes to unusually high metamorphic grade, upper amphibolite facies, at Cemetery Ridge. Coin 21 mm. **(B)** Morb affinity of PORS metabasalt. **(C)** Most common type of chondrite-normalized (Pourmand et al. 2012) REE spectra of PORS metabasalt (Haxel et al. 1987; Dawson and Jacobson 1989; Strickland et al. 2018).

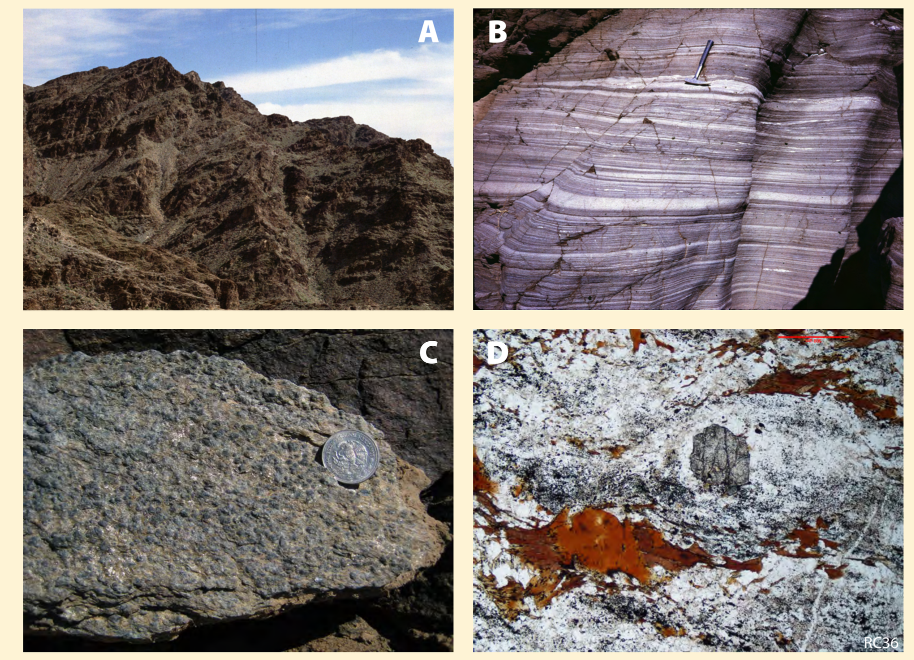

Figure 2. Orocopia quartzofeldspathic schist. **(A)** Stack of homogeneous schist; Gavilan Hills, southeast California. **(B)** Lithologic layering—transposed sedimentary bedding—parallel to foliation; Trigo Mountains, southwest Arizona. **(C)** Porphyroblasts of bluish-grey graphitic plagioclase, on weathered foliation surface of quartzofeldspathic schist; Cemetery Ridge, southwest Arizona. Coin 33 mm. **(D)** Biotite and garnet, with quartz, oligoclase or andesine, K-feldspar, and graphite; Cemetery Ridge. PPL, WOV 2.3 mm.

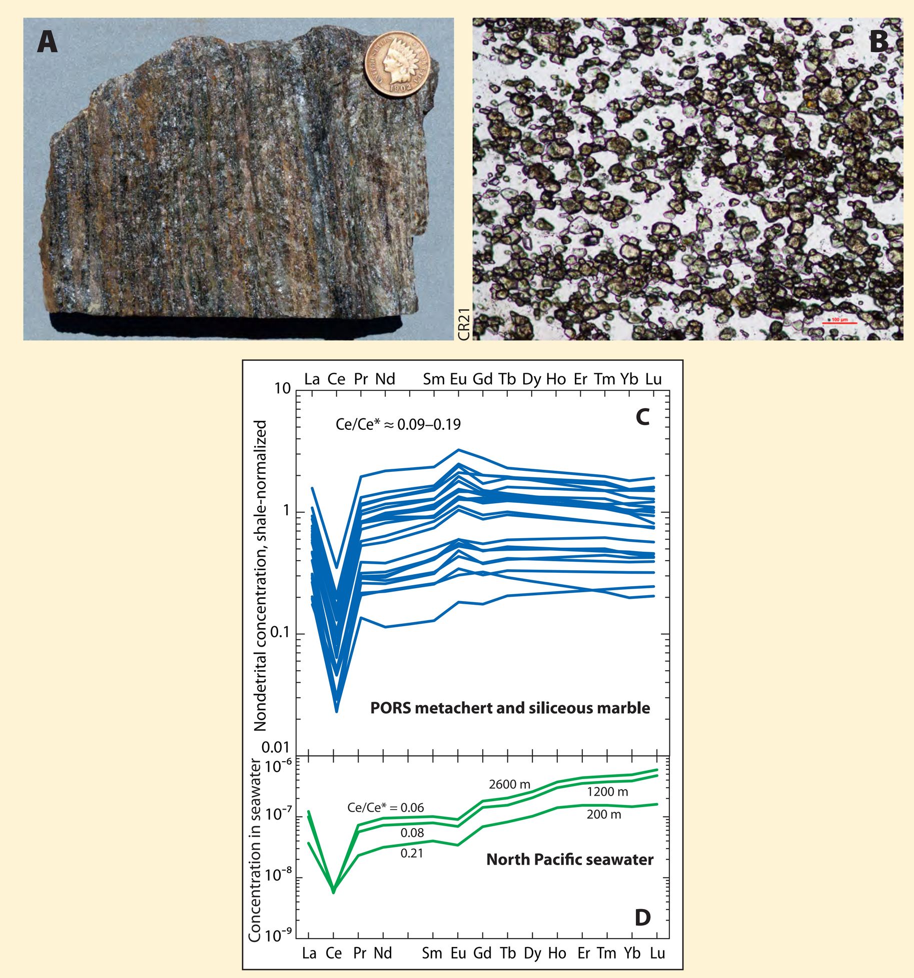

Figure 4. Ferromanganiferous metachert and siliceous marble. **(A)** Finely layered Fe-Mn metachert (spessartine-magnetite quartzite): mostly quartz, with thin yellowish layers of quartz plus spessartine and thin orangish layers of quartz plus limonite after magnetite; Orocopia Schist, Cemetery Ridge, southwest Arizona. Coin 19 mm. **(B)** Spessartine-rich layer; colorless matrix is quartz. PPL, WOV 1.2 mm. **(C)** REE spectra of metachert and siliceous marble, PORS, southern California and southwest Arizona (Haxel et al. 2021). Ce* = Ce extrapolated (logarithmically) between La and Pr. **(D)** REE in North Pacific seawater, for three shelf to bathyal depths (Alibo and Nozaki 1999). Upper and lower graphs differ in vertical scale by a factor of two. In both REE concentrations are shale normalized (Pourmand et al. 2012).

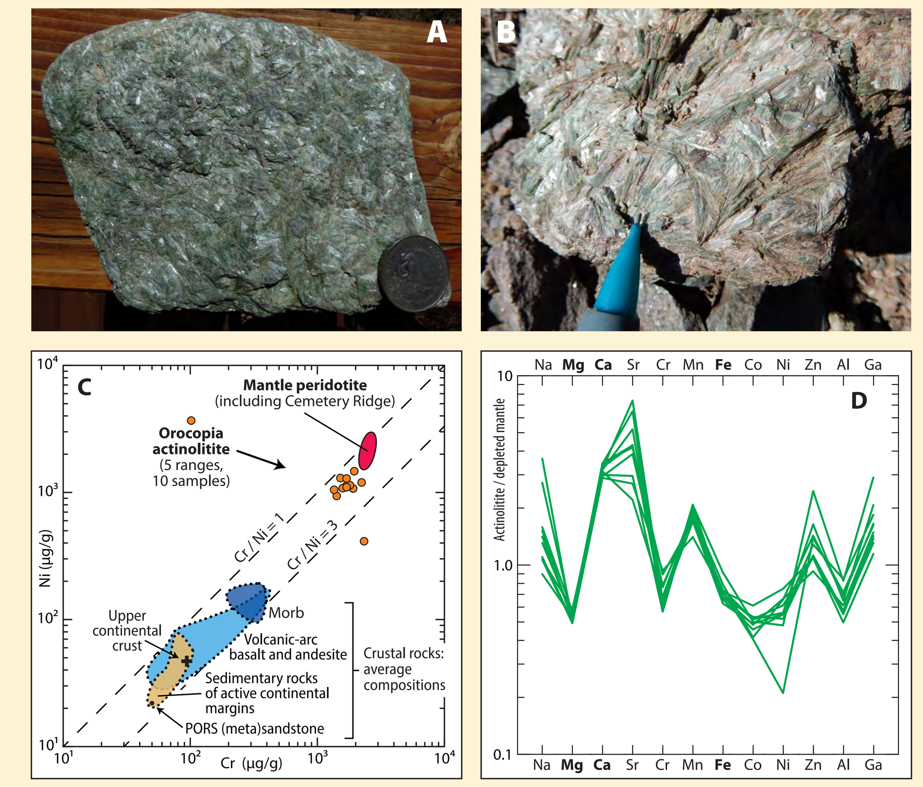

Figure 5. Actinolitite. **(A, B)** Actinolite pods in Orocopia Schist: Gavilan Hills, southeast California (A; coin 33 mm); Plomosa Mountains, southwest Arizona (B; WOV ≈ 8 cm). **(C)** Enrichment of Cr and Ni in actinolitite. Field of mantle peridotite includes primitive and depleted mantle. **(D)** Major and trace element concentrations in Orocopia actinolitite in five mountain ranges, southeast California and southwest Arizona; normalized to depleted mantle (Salters and Stracke 2004). Among the three essential elements (bold), congruence of Ca is required by stoichiometry of actinolite, whereas Mg and Fe could vary widely but do not: MgO/(MgO+FeO*) = 0.85 ± 0.03.

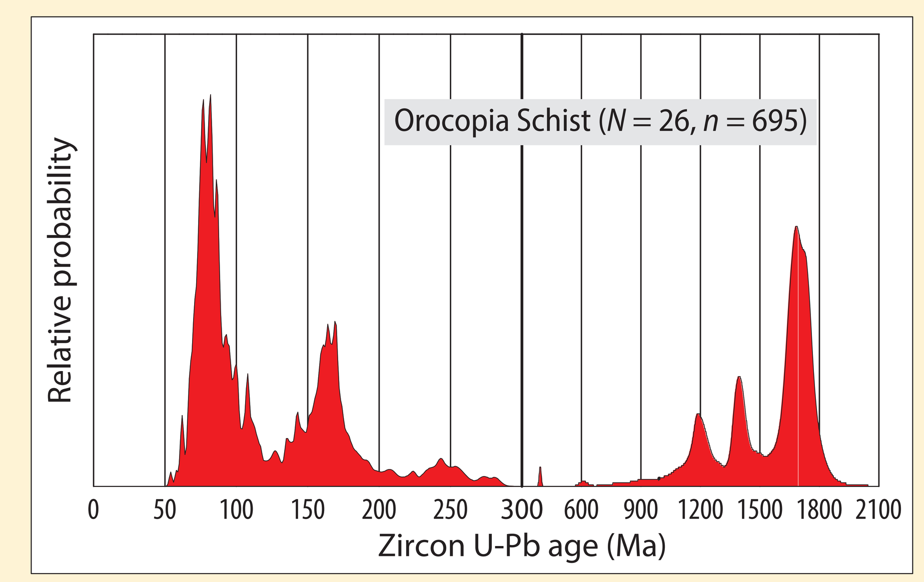

Figure 6. Probability distributions for age of detrital zircon in Orocopia Schist in southeast California and southwest Arizona; excluding Cemetery Ridge, where detrital zircon is accompanied by considerable young metamorphic zircon (Jacobson et al. 2017). *N*, number of samples; *n*, number of analyses. Horizontal scale changes at 300 Ma; vertical scales on either side of break differ such that equal area represents equal probability.

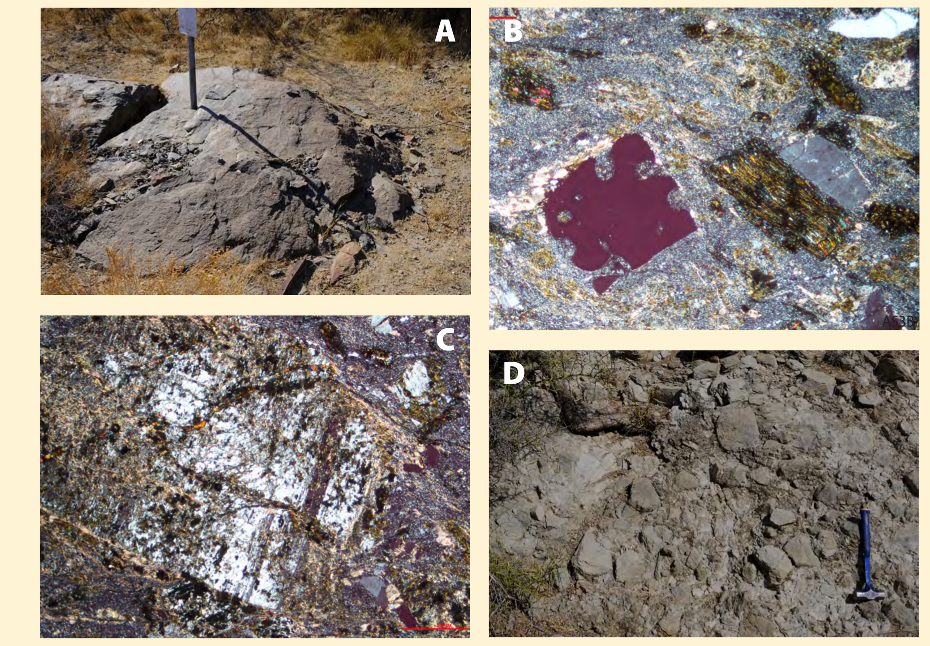

Figure 7. "Alamo schist"; purported Orocopia Schist. **(A)** Roadside block (≈ 1.5 m across) of dark-gray metarhyolite, with shiny sericitic foliation; sampled by Elliott and Corones (2019). **(B, C)** Phenocrysts in dark metarhyolite: embayed bipyramidal quartz (near extinction; magenta color is artifactual) and euhedral biotite largely altered to chlorite; plagioclase, heavily altered to calcite and sericite, with relict albite twinning. Phenocrysts are entirely uncharacteristic of Orocopia quartzofeldspathic schist, a thoroughly recrystallized *metasedimentary* rock. Turbid groundmass is largely quartz, calcite, and sericite. XP; WOV 4.3, 3.1 mm. **(D)** Breccia derived from metamorphosed rhyolitic lithic tuff or tuffaceous sandstone. Images A and D by Richard Hereford.

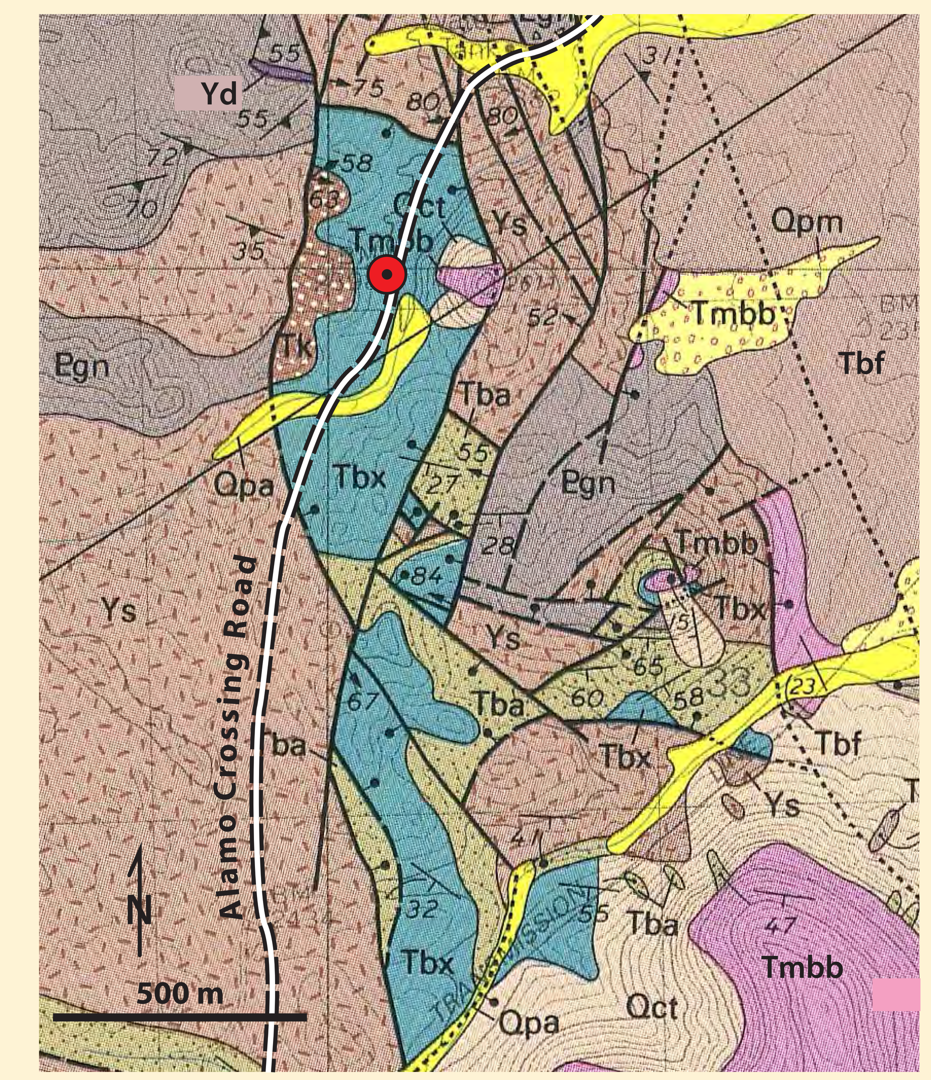

Figure 8. Geologic map of Miocene megabreccia (Tbx, blue) and surrounding rocks, west-central part of Signal 7.5-minute quadrangle, west-central Arizona (Lucchitta and Suneson 1994). Red dot marks "Alamo schist" locality. Other major units: Qct, colluvium and talus; Tbf, conglomerate ('basin fill'); Tmbb, basaltic andesite; Tk, arkosic conglomerate and sandstone; Tba, (basal) arkosic conglomerate; Yd, Ys, Ꝑgn—Proterozoic crystalline rocks. Local Oligocene to Miocene stratigraphic sequence (oldest to youngest): Tba, Tbx, Tk, Tmbb, Tbf.

References Cited

Alibo, D.S., and Nozaki, Y., 1999, Rare earth elements in seawater: Particle association, shale-normalization, and Ce oxidation: Geochimica et Cosmochimica Acta, v. 63, p. 363–372.

Bryant, B., 1995, Geologic map, cross sections, isotopic dates, and mineral deposits of the Alamo Lake 30′ × 60′ quadrangle, west-central Arizona: U.S. Geological Survey Map I-2489, scale 1:100,000.

Chapman, A.D., 2016, The Pelona-Orocopia-Rand and related schists of southern California: a review of the best-known archive of shallow subduction on the planet: International Geology Review, v. 59, p. 664–701.

Dawson, M.R., and Jacobson, C.E., 1989, Geochemistry and origin of mafic rocks from the Pelona, Orocopia, and Rand Schists, southern California: Earth and Planetary Science Letters, v. 92, p. 371–385.

Elliott, W.J., and and Corones, J.L., 2019, Alamo schist north of Alamo Lake, Arizona, *in* Miller, D. M., ed., Exploring ends of eras in the eastern Mojave Desert: Desert Symposium Field Guide and Proceedings, April 2019, p. 128–133.

Grove, M., Jacobson, C.E., Barth, A.P., and Vucic, A., 2003, Temporal and spatial trends of Late Cretaceous–early Tertiary underplating of Pelona and related schist beneath southern California and southwestern Arizona, *in* Johnson, S.E., Patterson, S.R., Fletcher, J.M., Girty, G.H., Kimbrough, D.L., and Martin-Barajas, A., eds., Tectonic evolution of northwestern Mexico and the southwestern USA: Geological Society of America Special Paper 374, p. 381–406.

Haxel, G.B., and Dillon, J.T., 1978, The Pelona-Orocopia Schist and Vincent-Chocolate Mountain thrust system, southern California, *in* Howell, D.G., and McDougall, K.A., eds., Mesozoic paleogeography of the western United States: Pacific Section, Society of Economic Paleontologists and Mineralogists, Pacific Coast Paleogeography Symposium 2, p. 453–469.

Haxel, G.B., Budahn, J.R., Fries, T.L., King, B.W., White, L.D., and Aruscavage, P.J., 1987, Geochemistry of the Orocopia Schist, southeastern California: Summary, *in* Dickinson, W.R., and Klute, M.A., eds., Mesozoic rocks of southern Arizona and adjacent areas: Arizona Geological Society Digest v. 18, p. 49–64.

Haxel, G.B., Jacobson, C.E., Richard, S.M., Tosdal, R.M., and Grubensky, M.J., 2002, The Orocopia Schist in southwest Arizona: early Tertiary oceanic rocks trapped or transported far inland, *in* Barth, A., ed., Contributions to crustal evolution of the southwestern United States: Geological Society of America Special Paper 365, p. 99–128.

Haxel, G.B., Jacobson, C.E., and Wittke, J.H., 2015, Mantle peridotite in newly discovered far-inland subduction complex, southwest Arizona: initial report: International Geology Review, v. 57, p. 871–892.

Haxel, G.B., Beard, L.S., and Jacobson, C.E., 2018a, Significance of northeast-southwest orientation of prograde lineation in the Pelona-Orocopia-Rand-Schist low-angle subduction complex, southern California and southwest Arizona: Geological Society of America Abstracts with Programs, v. 50, no. 5, # 313363.

Haxel, G.B., Wittke, J.H., Epstein, G.S., and Jacobson, C.E., 2018b, Serpentinization-related nickel, iron, and cobalt sulfide, arsenide, and intermetallic minerals in an unusual inland tectonic setting, southern Arizona, USA, *in* Ingersoll, R.V., Graham, S.A., and Lawton, T.F., eds., Tectonics, sedimentary basins, and provenance: A celebration of the career of William R. Dickinson: Geological Society of America Special Paper 540, p. 65–86.

Haxel, G.B., Epstein, G.S., Jacobson, C.E., Wittke, J.H., Standlee, K.G., and Mulligan, S.R., 2021, Geologic map of peridotite and associated metasomatic rocks in the Orocopia Schist subduction channel (latest Cretaceous) at Cemetery Ridge, southwest Arizona: Arizona Geological Survey Contributed Report, in press, map scale 1:2000.

Jacobson, C.E., Dawson, M.R., and Postlethwaite, C.E., 1988, Structure, metamorphism, and tectonic significance of the Pelona, Orocopia, and Rand Schists, southern California, *in* Ernst, W. G., ed., Metamorphism and crustal evolution of the western United States (Rubey Volume VII): Prentice-Hall, p. 976–997.

Jacobson, C.E., Grove, M., Vućić, A., Pedrick, J.N., and Ebert, K.A., 2007, Exhumation of the Orocopia Schist and associated rocks of southeastern California: Relative roles of erosion, synsubduction tectonic denudation, and middle Cenozoic extension, *in* Cloos, M., Carlson, W.D., Gilbert, M.C., Liou, J.G., and Sorensen, S.S., eds., Convergent margin terranes and associated regions: A tribute to W.G. Ernst: Geological Society of America Special Paper 419, p. 1–37.

Jacobson, C.E., Grove, M., Pedrick, J.N., Barth, A.P., Marsaglia, K.M., Gehrels, G.E., and Nourse, J.A., 2011, Late Cretaceous-early Cenozoic tectonic evolution of the southern California margin inferred from provenance of trench and forearc sediments: Geological Society of America Bulletin, v. 123, p. 485–506.

Jacobson, C.E., Hourigan, J.K., Haxel, G.B., and Grove, M., 2017, Extreme latest Cretaceous–Paleogene low-angle subduction: Zircon ages from Orocopia Schist at Cemetery Ridge, southwestern Arizona, USA: Geology, p. 951–954.

Lucchitta, I., and Suneson, N.H., 1989, Stratigrahic section of the Castaneda Hills–Signal area, Arizona, *in* Sherrod, D.R., and Nielson, J.E., eds., Tertiary stratigraphy of highly extended terranes, California, Arizona, Nevada: U.S. Geological Survey Bulletin 2053, p. 139–144.

Lucchitta, I, and Suneson, N.H., 1994, Geologic map of the Signal quadrangle, Mohave County, Arizona: U.S. Geological Survey Map GQ-1709, scale 1:24,000.

Pourmand, A., Dauphas, N., and Ireland, T.J., 2012, A novel extraction chromatography and MC-ICP-MS technique for rapid analysis of REE, Sc and Y: Revising CI-chondrite and Post-Archean Australian Shale (PAAS) abundances: Chemical Geology, v. 291, p. 38–54.

Salters, V.J.M., and Stracke, A., 2004, Composition of the depleted mantle: Geochemistry, Geophysics, Geosystems, v. 5, 2003GC000597

Seymour, N.M., Strickland, E.D., Singleton, J.S., Stockli, D.F., and Wong, M.S., 2018, Laramide subduction and metamorphism of the Orocopia Schist, northern Plomosa Mountains, west-central Arizona: Insights from zircon U-Pb geochronology: Geology, v. 46, p. 847–850.

Spencer, J.E., and Reynolds, S.J., 1989a, Middle Tertiary tectonics, *in* Jenny, J.P., and Reynolds, S.J., eds., Geologic evolution of Arizona: Arizona Geological Society Digest 17, p. 539–574.

Spencer, J.E., and Reynolds, S.J., 1989b, Tertiary structure, stratigraphy, and tectonics of the Buckskin Mountains, *in* Spencer, J.E., and Reynolds, S.J., eds., Geology and mineral resources of the Buckskin and Rawhide Mountains, west-central Arizona: Arizona Geological Survey Bulletin 198, p. 103–167.

Spencer, J.E., Grubensky, M.J., Duncan, J.T., Shenk, J.D., Yarnold, J.C., and Lombard, J.P., 1989, Geology and mineral deposits of the central Artillery Mountains, *in* Spencer, J.E., and Reynolds, S.J., eds., Geology and mineral resources of the Buckskin and Rawhide Mountains, west-central Arizona: Arizona Geological Survey Bulletin 198, p. 168–189.

Spencer, J.E., and Reynolds, S.J., 1990, Relationship between Mesozoic and Cenozoic tectonic features in west-central Arizona and adjacent southeastern California: Journal of Geophysical Research: Solid Earth, v. 95, p. 539–555.

Strickland, E.D., Singleton, J.S., Griffin, A.T.B., and Seymour, N.M., 2017, Geologic map of the northern Plomosa Mountains metamorphic core complex, Arizona: Arizona Geological Survey Contributed Map 17-A, scale 1:10,000.

Strickland, E.D., Singleton, J.S., and Haxel, G.B., 2018, Orocopia Schist in the northern Plomosa Mountains, west-central Arizona: A Laramide subduction complex exhumed in a Miocene metamorphic core complex: Lithosphere, v. 10, p. 723–742.

Yarnold, J.C., 1989, Middle Tertiary stratigraphy of the northern Rawhide Mountains and Artillery Mountains, Arizona, *in* Sherrod, D.R., and Nielson, J.E., eds., Tertiary stratigraphy of highly extended terranes, California, Arizona, Nevada: U.S. Geological Survey Bulletin 2053, p. 145–150.

Yarnold, J.C., and Lombard, J.P., 1989, A facies model for large rock-avalanche deposits formed in dry climates, *in* Colburn, I.P., Abbott, P.L., and Minch, J., eds., Conglomerates in basin analysis: A symposium dedicated to A.O., Woodford: Pacific Section, Society of Economic Paleontologists and Mineralogists, v. 62, p. 9–31.

April 2021; Flagstaff, AZ

Text: Garamond Premier Pro, Medium Subhead, 24/29. Headings: GPP, Bold Subhead, 28/34. Captions: Myriad Pro, 21/25.